ELSEVIER

Journal of Organometallic Chemistry 641 (2002) 165–172

Journal of Organometallic Chemistry

www.elsevier.com/locate/jorganchem

# Supported organometallic complexes
# Part XXX. Hydroformylation of 1-hexene in interphases — the influence of different kinds of inorganic–organic hybrid co-condensation agents on the catalytic activity[☆]

Ekkehard Lindner *, Thomas Salesch, Stefan Brugger, Frank Hoehn, Peter Wegner, Hermann A. Mayer

*Institut für Anorganische Chemie der Universität Tübingen, Auf der Morgenstelle 18, D-72076 Tübingen, Germany*

Received 25 July 2001; accepted 10 August 2001

---

**Abstract**

A novel mono-T-silyl functionalized triphenylphosphine ligand was prepared by a simple coupling reaction of (*p*-aminophenyl)diphenylphosphine and 3-triethoxysilylpropylisocyanate. The corresponding carbonylchlorobisphosphinerhodium(I) complex $ClRh(CO)[PPh_2C_6H_4NHCONH(CH_2)_3Si(OEt)_3]_2$ was synthesized in order to be sol–gel processed with various amounts of different D- and T-silyl bifunctionalized co-condensation agents. The polysiloxane matrices and the active rhodium centers were investigated by means of multinuclear solid state NMR ($^{13}C$, $^{29}Si$, $^{31}P$) and dynamic NMR measurements. The rhodium containing xerogels were applied in the hydroformylation of 1-hexene. These stationary phases show remarkable catalytic activities independent on the solvent. An enhancement of the activities is achieved when T-silyl bifunctionalized co-condensation agents are used to build up the carrier matrix. © 2002 Elsevier Science B.V. All rights reserved.

*Keywords:* Sol–gel proccess; Supported complexes; Rhodium(I); Hydroformylation; Solid state NMR spectroscopy

---

## 1. Introduction

The anchoring of reactive centers, in particular catalytically active transition metal complexes, to an inert support is a field of increasing interest in terms of academic as well as commercial research [2–9]. Such materials are able to combine the advantages of homogenous and heterogeneous catalysis: the catalyst becomes easily separable from the reaction products and it can be reused in several runs without an essential loss of activity. On the other hand, the reactive centers are well defined and the improvement of their properties is not only empirical. Due to the homogenous character of the catalytic reaction the activities and selectivities are high [10].

However, there are still specific problems with such systems which inhibited the commercial breakthrough of these types of catalysts. They can leach from the support during the catalytic reaction. Furthermore the heterogenization of complexes leads to reduced mobility of the reactive centers causing lower activities and selectivities of the anchored catalysts compared to their homogenous counterparts [11].

A versatile approach to reduce or even eliminate these problems is the introduction of the concept of interphase [12]. In the presence of a stationary phase (e.g. an anchored metal complex) and a mobile phase (solvent, gaseous or liquid reactant) a penetration of both phases on a molecular level takes place. This state is designated as ‘interphase’ since no homogenous phase is formed. However, interphases are able to imitate homogenous conditions providing favorable activities in different types of catalytic reactions without any essential metal leaching. A typical approach for the generation of stationary phases in interphase chemistry

---

[☆] Part XXIX, see Ref. [1].

[*] Corresponding author. Tel.: +49-7071-29-72039; fax: +49-7071-29-5306.

*E-mail address:* ekkehard.lindner@uni-tuebingen.de (E. Lindner).

PII: S0022-328X(01)01313-4

is the sol–gel process, which offers a convenient route for the preparation of suitable polysiloxane networks under smooth and low temperature conditions. Simultaneous co-condensation of T-silyl functionalized metal complexes or ligands with various alkoxysilanes or organosilanes provides materials, in which the reactive centers are nearly homogeneously distributed across a chemical and thermal inert carrier matrix [13–20]. Since the polysiloxane-bound active centers are readily accessible even for larger molecules, those kinds of inorganic–organic hybrid materials are predestinated for catalytic reactions [21–25].

Due to this fact we transferred the concept of interphase to hydroformylation, which is one of the most important industrial catalytic processes. For this aim a novel T-silyl functionalized triphenylphosphine ligand was prepared, introducing the spacer unit in the *para*-position of only one phenyl ring. Subsequently the catalytically active T-silyl functionalized carbonylchloro[bis(phosphine)]rhodium(I) complex was synthesized. The ligand as well as the Vaska-analogous rhodium(I) complex were condensed into matrices built by various D- and T-silyl bifunctionalized co-condensation agents [20,26]. Structural investigations of these novel stationary phases were carried out by multinuclear solid state NMR spectroscopy. To study the mobility of the matrices and active centers detailed dynamic solid state NMR measurements were undertaken. The mobility of the rhodium containing xerogels were compared with the dynamics of the sol–gel processed phosphine prior to the employment of these complexes in the hydroformylation of 1-hexene.

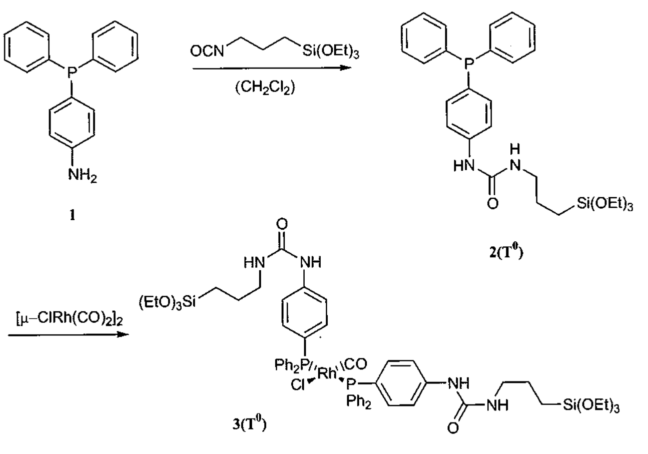

Scheme 1.

Table 1
Labeling of the compounds

| Precursor | Co-condensation agent | Ideal T/D or T/T ratio | Xerogel |
|---|---|---|---|
| **2(T$^0$)** | **4(D$^0$)** | 1:5 | **X2a** |
| **2(T$^0$)** | **5(D$^0$)** | 1:5 | **X2b** |
| **3(T$^0$)** | **4(D$^0$)** | 1:20 | **X3a** |
| **3(T$^0$)** | **5(D$^0$)** | 1:20 | **X3b** |
| **3(T$^0$)** | **4(T$^0$)** | 1:20 | **X3c** |
| **3(T$^0$)** | **5(T$^0$)** | 1:20 | **X3d** |

## 2. Results and discussion

### 2.1. Synthesis of the T-silyl functionalized ligand 2(T$^0$) and of the monomeric rhodium(I) complex 3(T$^0$)

The triphenylphosphine analogous ligand **2(T$^0$)** was obtained in good yields as a waxy colorless solid by the reaction of (*p*-aminophenyl)diphenylphosphine (**1**) with one equivalent of triethoxysilylpropylisocyanate in dichloromethane. The modified Vaska complex **3(T$^0$)** can be easily prepared by the reaction of **2(T$^0$)** with a half equivalent of [μ-ClRh(CO)$_2$]$_2$ in benzene (Scheme 1). Both compounds were characterized by $^1$H-, $^{13}$C{$^1$H}-, $^{31}$P{$^1$H}-NMR, and IR spectroscopy, as well as mass spectrometry, and elemental analysis. In the $^{31}$P{$^1$H}- and $^{29}$Si{$^1$H}-NMR spectra of **2(T$^0$)** each one signal is observed at $\delta = -5.5$ and $-45.1$, respectively. Compared to triphenylphosphine the *para*-positioned spacer function exerts nearly no influence on the chemical shift of the $^{31}$P nucleus in **2(T$^0$)**. The composition of the rhodium complex **3(T$^0$)** was corroborated by its EIMS showing the molecular peak at $m/z = 1214$. Only one doublet with a $^1J_{\mathrm{RhP}}$ coupling constant of 124.7 Hz occurs in the $^{31}$P{$^1$H}-NMR spectrum of complex **3(T$^0$)**, which is indicative of a *trans*-position of the phosphine ligands [27]. A characteristic absorption at 1980 cm$^{-1}$ in the IR spectrum of **3(T$^0$)** is assigned to the carbonyl stretching vibration. Other analytic data are summarized in the experimental part.

### 2.2. Sol–gel processing of 2(T$^0$) and 3(T$^0$)

The xerogels **X2a** and **X2b** were prepared by sol–gel processing of the monomeric T-silyl functionalized ligand **2(T$^0$)** with the co-condensation agent **4(D$^0$)** and **5(D$^0$)**, respectively. In the case of **X3a–d** the rhodium complex **3(T$^0$)** was condensed into a matrix consisting of the co-condensation agents **4(D$^0$)**, **4(T$^0$)**, **5(D$^0$)**, and **5(T$^0$)** (Table 1, Scheme 2). The properties of such materials strongly depend on the reaction conditions during the entire sol–gel process such as concentration of the monomers, type of solvent, temperature, and kind of catalyst. All sol–gel processes were carried out in THF with an excess of water and tetrabutylammoniumfluoride as catalyst. To guarantee reproducible materials uniform reaction conditions were maintained.

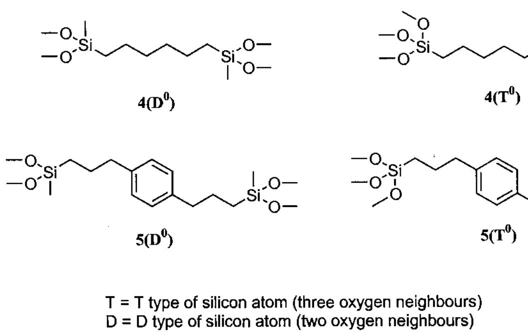

Scheme 2.

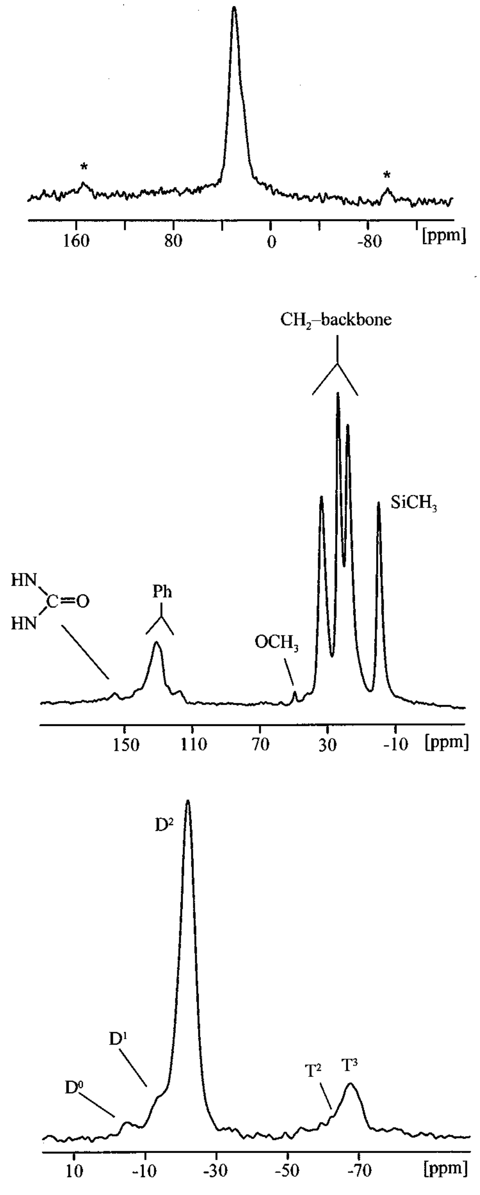

Fig. 1. Solid state NMR spectra; top: $^{31}$P CP/MAS of **X3d**; middle: $^{13}$C CP/MAS of **X2a**; bottom: $^{29}$Si CP/MAS of **X3a** (* rotational side bands).

### 2.3. Solid state NMR spectroscopic investigations

Due to the amorphous nature of these materials, solid state NMR spectroscopy plays an important role in investigating the structure and the dynamic behavior of xerogels [28–30]. $^{29}$Si-NMR spectroscopy enables the characterization of the carrier matrix and the degree of condensation. $^{13}$C- and $^{31}$P CP/MAS-NMR spectroscopy allows an insight into the hydrocarbon regions and the reactive center, respectively (Fig. 1).

#### 2.3.1. $^{29}$Si CP/MAS-NMR spectroscopy and mobility of the matrix

As a result of an incomplete condensation the $^{29}$Si CP/MAS-NMR spectra of the above-mentioned xerogels reveal signals of various substructures with corresponding $D^i$- and $T^n$-functions. Typical chemical shifts are $\delta = -4.8$ ($D^0$), $-14.3$ ($D^1$), $-22.3$ ($D^2$), $-58.2$ ($T^2$), and $-67.7$ ($T^3$). They remain unchanged with respect to the stoichiometric composition of the materials and the kind of co-condensate. All silicon atoms in the polysiloxane matrix are in direct proximity of protons, thus silyl species are detectable via cross polarization [31,32]. Therefore the degree of condensation of D- and T-silyl functions were determined by contact time variation experiments (Table 2) [20,33]. However, due to the very low concentration of the T-groups in the xerogels **X3a** and **X3b** they can hardly be detected. Therefore the quantification of these silyl functions with contact time variation experiments is not feasible within a reasonable time and hence was carried out by deconvolution of the $^{29}$Si CP/MAS spectra. In all above-mentioned xerogels the degrees of condensation range from 74 to 92% and 90 to 96% for the D- and T-groups, respectively. These results are in agreement with former investigations [34,35].

In the solid state the T/D-materials do not differ significantly in the cross polarization constant $T_{\mathrm{SiH}}$ and the relaxation time $T_{1\rho\mathrm{H}}$ (via $^{29}$Si) indicating that the mobilities of the matrices in **X2a**, **b** and **X3a**, **b** are similar. The T/T-polymers **X3c** and **X3d** show differences in the $T_{\mathrm{SiH}}$ values. In both materials the number and distance of the protons surrounding the $^{29}$Si nucleus is very similar which means that the cross polarization constant $T_{\mathrm{SiH}}$ is only governed by the mobility. The higher $T_{\mathrm{SiH}}$ values of **X3c** indicate a more inefficient transfer of the magnetization of the protons to the $^{29}$Si atoms than in **X3c** and thus a slightly faster motion.

#### 2.3.2. $^{31}$P CP/MAS-NMR spectroscopy and mobility of the reactive center

In the $^{31}$P CP/MAS-NMR spectra of the polysiloxane-bound phosphines **X2a**, **b** one signal is observed at $-6.3$ and $-6.7$ ppm, respectively. Also, only one broad signal with a chemical shift at about 29 ppm

Table 2
Relative $I_0$, $T_{SiH}$, and $T_{1\rho H}$ data of the silyl species in the xerogels

| Xerogel | Relative $I_0$ data of D and T species [a] | | | | | Degree of condensation (%) | | $T_{SiH}$ (ms) [b] | | | | | $T_{1\rho H}$ (ms) [c] |
|---|---|---|---|---|---|---|---|---|---|---|---|---|---|
| | $D^0$ | $D^1$ | $D^2$ | $T^2$ | $T^3$ | D | T | $D^0$ | $D^1$ | $D^2$ | $T^2$ | $T^3$ | |
| **X2a** | 1.5 | 17.4 | 100 | 6.1 | 20.8 | 92 | 93 | [d] | [d] | 1.24 | [d] | 1.43 | 7.1 |
| **X2b** | 2.0 | 16.1 | 100 | 2.6 | 18.7 | 92 | 96 | [d] | [d] | 1.45 | [d] | 1.83 | 6.8 |
| **X3a** | [e] | 100 [f] | 91.3 [f] | 1.3 [f] | 3.9 [f] | 74 | 95 | [e] | 1.02 | 1.28 | [d] | 1.11 | 6.3 |
| **X3b** | [e] | 55.2 [f] | 100 [f] | 1.6 [f] | 8.6 [f] | 82 | 95 | [e] | 0.96 | 1.22 | [d] | 1.15 | 5.8 |
| **X3c** | [e] | [e] | [e] | 31.6 | 100 | | 91 | [e] | [e] | [e] | 1.15 | 2.02 | 6.0 |
| **X3d** | [e] | [e] | [e] | 42.2 | 100 | | 90 | [e] | [e] | [e] | 0.67 | 1.52 | 5.1 |

[a] $I_0$ values calculated according to Ref. [19].

[b] Determined by contact time variation.

[c] Determined via $^{29}$Si-NMR with the experiment according to Ref. [39].

[d] Intensity to low for a precise determination of $T_{SiH}$.

[e] Species not detectable.

[f] Determined via deconvolution of $^{29}$Si CP/MAS-NMR spectra ($T_c = 5$ ms).

occurs in the $^{31}$P CP/MAS-NMR spectra of the rhodium containing polymers **X3a**–**d**. These results remind of the ligand and the monomeric rhodium(I) complex measured in solution. No other phosphine species is detectable in the freshly synthesized polymers, but exposure to air for some hours leads to the formation of phosphine oxide.

Due to higher values of the cross polarization constant $T_{PH}$ (Table 3) the reactive centers (free phosphine ligand) in **X2a** and **X2b** show an enhanced mobility compared to the polysiloxane-bound rhodium complexes in **X3a**–**d**. Obviously the P-coordination of the ligands enables a fast magnetization transfer for all types of co-condensates. Furthermore it can be demonstrated, that the rhodium(I) centers in the T/D-materials **X3a**, **b** are slightly more mobile than those in the T/T-polymers **X3c**, **d**. These results are in a good agreement with former investigations [20,35].

### 2.3.3. $^{13}$C CP/MAS-NMR spectroscopy

The $^{13}$C CP/MAS-NMR spectra of **X2a**, **X3a**, and **X3c** reveal a broad group of signals in the aromatic region, which stems from the phenyl carbon atoms of the functionalized phosphine ligand. The aliphatic region is dominated by three and four major signals, respectively, which are assigned to the hydrocarbon chain of the co-condensate. In the case of the hybrid polymers **X2b**, **X3b**, and **X3d** all main signals can be traced back to the backbone of the matrix. It is noteworthy, that the signal occurring at about 155 ppm in each $^{13}$C CP/MAS-NMR spectrum is attributed to the urea function in the spacer. The weak or missing peaks for the alkoxysilyl substituent indicate a rather high degree of hydrolysis.

### 2.4. Hydroformylation of 1-hexene in the interphase

Square-planar rhodium(I) complexes have been applied as catalysts for the hydroformylation of various olefins for more than three decades [36–38]. In this work the polysiloxane-bound rhodium(I) complexes **X3a**, **X3b**, **X3c**, and **X3d** were employed in the hydroformylation of 1-hexene with good turnover numbers (TON) in dichloromethane and toluene as solvents (Tables 4 and 5). In the case of dichloromethane a complete listing of the constituents of the reaction solution is presented in Fig. 2. Methanol, the most commonly solvent for catalytic hydroformylations, leads only to acetalyzation products when the above-mentioned catalysts were used, which could be demonstrated by $^1$H- and $^{13}$C{$^1$H}-NMR spectroscopy. It is remarkable, that the catalytic activity in toluene is higher than in dichloromethane. In the case of toluene a conversion of 1-hexene of 100% for the first run of each catalyst was achieved. This is in contrast compared to the swelling capabilities of the polymers in each solvent [26]. The selectivity does not change re-

Table 3
$T_{1\rho H}$ (via $^{31}$P) and $T_{PH}$ parameters of the xerogels

| Xerogel | $T_{1\rho H}$ [ms] [a] | $T_{PH}$ [ms] [b] |
|---|---|---|
| **X2a** | 8.3 | 2.05 |
| **X2b** | 6.5 | 1.94 |
| **X3a** | 4.6 | 0.52 |
| **X3b** | 7.4 | 0.48 |
| **X3c** | 10.8 | 0.32 |
| **X3d** | 6.9 | 0.29 |

[a] Determined via $^{31}$P according to Ref. [39].

[b] Determined via contact time variation.

Table 4
Hydroformylation of 1-hexene in toluene [a]

| Catalyst | Conversion (%) | Isomerization (%) | Hydroformylation (%) | *n*/(*n*+*iso*) | TON [b] | TOF [c] |
|---|---|---|---|---|---|---|
| **3(T$^0$)** | 100 | 17.4 | 82.6 | 0.57 | 13216 | 777 |
| **X3a** | 100 | 33.7 | 66.3 | 0.67 | 10608 | 624 |
| **X3b** | 100 | 20.9 | 79.1 | 0.58 | 12656 | 734 |
| **X3c** | 100 | 5.3 | 94.7 | 0.53 | 15152 | 891 |
| **X3d** | 100 | 7.5 | 92.5 | 0.53 | 14800 | 870 |

[a] Reaction conditions: 70 °C, 30 bar CO, 30 bar $H_2$, 1020 min, 30 ml solvent, 10 ml (80 mmol) 1-hexene, 5 µmol catalyst, ratio catalyst–substrate 1:16000.

[b] Turnover number: [mol (aldehyde)/mol (catalyst)].

[c] Turnover frequency: {mol (aldehyde)/[mol (catalyst)/h]}.

Table 5
Hydroformylation of 1-hexene in dichloromethane [a]

| Catalysts | Conversion (%) | Isomerization (%) | Hydroformylation (%) | *n*/(*n*+*iso*) | TON [b] | TOF [c] |
|---|---|---|---|---|---|---|
| **3(T$^0$)** | 66.5 | 27.7 | 72.3 | 0.69 | 7696 | 452 |
| **X3a** | 88.9 | 49.5 | 50.5 | 0.72 | 7184 | 423 |
| **X3b** | 69.3 | 30.7 | 69.3 | 0.69 | 7680 | 451 |
| **X3c** | 100 | 13.0 | 87.0 | 0.58 | 13920 | 819 |
| **X3d** | 100 | 23.9 | 76.1 | 0.65 | 12176 | 716 |

[a] Reaction conditions: 70 °C, 30 bar CO, 30 bar $H_2$, 1020 min, 30 ml solvent, 10 ml (80 mmol) 1-hexene, 5 µmol catalyst, ratio catalyst–substrate 1:16000.

[b] Turnover number: [mol (aldehyde)/mol (catalyst)].

[c] Turnover frequency: {mol (aldehyde)/[mol (catalyst)/h]}.

markably and is 0.62 ($\pm 0.1$) ($n/[n+iso]$) for all stationary phases. However, it was not the target of these investigations to get high yields of linear aldehydes with the simple and unspecific square-planar rhodium(I) complex. A remarkable influence of the TONs by a modification of the organic part from pure alkyl (**X3a**, **X3c**) to a chain with a phenylene unit (**X3b**, **X3d**) could not be observed. These results are in agreement with the NMR studies of the mobility of the pure polymers [26]. By variation of the silyl functionality in the co-condensation agents higher conversions, in particular in the case of dichloromethane could be detected. Co-condensation agents with T-silyl groups (**X3c**, **X3d**) show a higher catalytic activity than those, which are provided with D-silyl moieties (**X3a**, **X3b**). This result indicates that a higher cross-linkage of the polymer does not exert a negative influence on the accessibility of the reactive centers in the interphase at the described catalytic conditions. The lower mobility of the T-silyl functionalized co-condensation agents, which was observed by solid state and suspension NMR investigations [26], and the swelling capability of the polymers, are evidently not the significant criterions for the catalytic activity of the reactive centers. A comparison of similar D- and T-silyl bifunctionalized hybrid materials in the time domain of the NMR spectroscopy is probably unsuitable. Better comparable are results of mobility studies, which were derived by dynamic fluorescence spectroscopy [39]. These investigations revealed, that polymers with the co-condensation agent **4(T$^0$)**, which are including a fluorescence active fluorene molecule, possess a higher rotational mobility of fluorene than polymers made of **3(T$^0$)** in the time domain of the fluorescence spectroscopy.

Finally it is noteworthy that no leaching of the transition metal was detectable by atomic absorption spectrocopy.

## 3. Conclusions

A novel T-silyl functionalized triphenylphosphine **2(T$^0$)** was prepared by a simple coupling reaction of

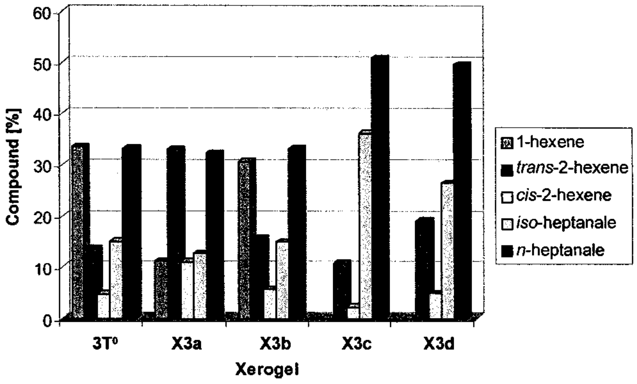

Fig. 2. Composition of the solution after hydroformylation of 1-hexene in dichloromethane.

(*p*-aminophenyl)diphenylphosphine (**1**) and 3-triethoxysilylpropylisocyanate. Treatment of the modified phosphine **2(T$^0$)** with [μ-ClRh(CO)$_2$] gave the T-silyl functionalized rhodium(I) complex **3(T$^0$)**. After sol–gel processing with different co-condensation agents the polymers were used in the hydroformylation of 1-hexene. Although the urea function in the spacer unit can represent a different possible reactive center, there was no evidence of disadvantage in the application of these kinds of materials in catalysis. For organometallic reactions in interphases with substrates that attack the urea unit (e.g. methyliodide) the ligand has to be changed into a system without any further functional group in the spacer unit [27].

With the application of different D- and T-silyl bifunctionalized co-condensation agents in the hydroformylation of 1-hexene these various stationary phases could be directly compared for the first time under catalytic conditions. Altogether a higher cross-linkage of polymers, which are provided with T-silyl bifunctionalized copolycondensates, is more advantageous under a pressure of 60 bar. The D-silyl bifunctionalized siloxanes, which are more mobile on the NMR time scale show a lower activity under these medium pressure conditions. Properties like the swelling capability and the mobility of the different parts of the polymer become less important. The accessibility of the reactive centers and thus the catalytic activity increase with the more rigid polymer backbone of T-silyl bifunctionalized co-condensation agents under the described conditions.

## 4. Experimental

### 4.1. Materials and instrumentation

Elemental analysis were carried out on a Vario EL Analyzer (Elementar Analytische Systeme Hanau). IR data were obtained on a Bruker IFS 48 FT-IR spectrometer. Solution nuclear magnetic resonance spectra were recorded on a Bruker DRX 250 spectrometer (field strength 5.87 T) at 296 K. Frequencies are as follows: $^1$H-NMR: 250.13 MHz (referenced to Me$_4$Si), $^{13}$C{$^1$H}-NMR: 62.90 MHz (referenced to Me$_4$Si), $^{29}$Si{$^1$H}-NMR: 49.96 MHz (referenced to Me$_4$Si), $^{31}$P{$^1$H}-NMR: 101.25 MHz (referenced to 85% H$_3$PO$_4$), MS: FD, Finnigan MAT 711A (8 kV, 333 K), EI, TSQ Finnigan (70 eV, 473 K) and reported as mass/charge ($m/z$).

CP/MAS solid state NMR spectra were recorded on Bruker DSX 200 multinuclear spectrometer equipped with a wide bore magnet (field strength 4.7 T). Magic angle spinning was applied at 10 kHz (4 mm ZrO$_2$ rotors) and 3–4 kHz (7 mm ZrO$_2$ rotors), respectively. Frequencies and standards: $^{31}$P-NMR: 81.961 MHz (4.7 T) [85% H$_3$PO$_4$, NH$_4$H$_2$PO$_4$ ($\delta = 0.8$) as second standard]; $^{13}$C-NMR: 50.228 MHz (4.7 T) [Me$_4$Si, carbonyl resonance of glycine ($\delta = 176.0$) as second standard]; $^{29}$Si-NMR: 39.73 MHz (4.7 T) (Q$_8$M$_8$ as second standard). All samples were packed under exclusion of molecular oxygen. The cross polarization constants $T_{\mathrm{XH}}$ were determined by variation of the contact time $T_c$ (14–16 experiments). The proton relaxation times in the rotating frame $T_{1\rho\mathrm{H}}$ were measured by direct proton spin lock-$\tau$-CP experiments [40] via $^{29}$Si-NMR and $^{31}$P-NMR. The relaxation parameters were obtained using Bruker software SIMFIT and WINFIT following the procedure described in Ref. [20].

All reactions and manipulations were carried out under Ar with the usual Schlenck techniques. Methanol was dried with magnesium and distilled prior to use. All other solvents were distilled from sodium benzophenone ketyl or calcium hydride. H$_2$O was distilled under inert gas prior to use. All solvents and reagents were stored under Ar. [μ-ClRh(CO)]$_2$ [41], (*p*-aminophenyl)diphenylphosphine (**1**) [42], and the co-condensation agents **4(D$^0$)**, **4(T$^0$)**, **5(D$^0$)**, and **5(T$^0$)** [20,26] were synthesized as described previously.

### 4.2. Catalysis

The hydroformylation experiments were carried out in a 100 ml stainless steel autoclave equipped with a mechanical stirring bar. The autoclave was flushed with Ar prior to the introduction of the reaction mixture (5 μmol of catalyst with respect to rhodium, 80 mmol of 1-hexene, and 30 ml of the solvent). The reaction mixture was set under CO pressure and stirred for 30 min prior to hydrogen introduction. After stirring for 5 min the mixture was heated to the required temperature. The quantitative analyses were performed on a GC 6000 Vega Series 2 (Carlo Erba Instruments) with an FID and a capillary column CP Sil 88 [17 m, carrier gas helium (50 kPa); integrator Hewlett Packard 3390 A]. Leaching investigations were carried out with a Varian Spectr AA 20 Plus atomic absorption spectrometer.

### 4.3. *N-[p-(Diphenylphosphinyl)phenyl]-N′-[(triethoxysilyl)propyl]urea* [**2(T$^0$)**]

To a solution of **1** (12.6 g, 45.4 mmol) in 30 ml of CH$_2$Cl$_2$ a solution of triethoxysilylpropylisocyanate (11.2 g, 45.4 mmol) in 10 ml of CH$_2$Cl$_2$ was slowly added. After stirring overnight the solvent was reduced in vacuum and **2(T$^0$)** was obtained as a colorless waxy solid which is sensitive to moisture and air. Yield: 21.3 g (89.4%) — $^1$H-NMR (CDCl$_3$): $\delta = 7.69–7.05$ (m, 14H, H-phenyl), 3.67 (q, $^3J_{\mathrm{HH}} = 6.91$ Hz, 6H, O–C*H*$_2$–CH$_3$), 3.08 (m, 2H, NH–C*H*$_2$–CH$_2$), 1.51 (m, 2H, CH$_2$–C*H*$_2$–CH$_2$), 1.11 (t, $^3J_{\mathrm{HH}} = 6.91$ Hz, 9H, O–CH$_2$–C*H*$_3$), 0.52 (m, 2H, CH$_2$–C*H*$_2$–Si) —

$^{13}$C{$^{1}$H}-NMR (CDCl$_3$): $\delta = 156.1$ (s, NH–CO–NH), 140.6–119.2 (m, C-phenyl), 58.5 (s, O–*C*H$_2$–CH$_3$), 42.7 (s, NH–*C*H$_2$–CH$_2$), 23.7 (CH$_2$–*C*H$_2$–CH$_2$), 18.4 (s, O–CH$_2$–*C*H$_3$), 7.8 (s, CH$_2$–*C*H$_2$–Si) — $^{31}$P{$^{1}$H}-NMR (CDCl$_3$): $\delta = -5.5$ — $^{29}$Si{$^{1}$H}-NMR (C$_6$D$_6$): $\delta = -45.1$ — IR (KBr, cm$^{-1}$): 3311 [$\nu$(NH)], 1643 [$\nu$(CO)] — MS (FD); *m*/*z*: 524 [M$^{+}$] — Anal. Found: C, 64.71; H, 6.90; N, 5.07. Calc. for $C_{28}H_{37}N_2O_4PSi$: C, 64.10; H, 7.11; N, 5.34%.

### 4.4. Chlorocarbonyl-bis{N-[p-(diphenylphosphinyl)-phenyl]-N′-[(triethoxysilyl)propyl]urea} rhodium(I) [3(T$^0$)]

To a solution of [μ-ClRh(CO)$_2$]$_2$ (0.24 g, 0.62 mmol) in 10 ml of benzene a solution of **2(T$^0$)** (1.31 g, 2.49 mmol) in 10 ml of benzene was added dropwise. The reaction mixture was stirred for 1 h at ambient temperature. The solvent was removed in vacuum and the residual waxy solid was dissolved in 10 ml of *n*-hexane. After stirring for 30 min the solvent was removed under reduced pressure and **3(T$^0$)** was obtained as a yellow microcrystalline solid which is sensitive to moisture and air. Yield: 1.49 g (98.4%) — $^{1}$H-NMR (CD$_2$Cl$_2$): $\delta = 7.97$–7.28 (m, 14H, H-phenyl), 3.71 (q, $^{3}J_{HH} = 7.22$ Hz, 6H, O–C*H*$_2$–CH$_3$), 3.03 (m, 2H, NH–C*H*$_2$–CH$_2$), 1.48 (m, 2H, CH$_2$–C*H*$_2$–CH$_2$), 1.11 (t, $^{3}J_{HH} = 7.22$ Hz, 9H, O–CH$_2$–C*H*$_3$), 0.52 (m. 2H, CH$_2$–C*H*$_2$–Si) — $^{13}$C{$^{1}$H}-NMR (CD$_2$Cl$_2$): $\delta = 156.0$ (s, NH–CO–NH), 143.0–118.1 (m, C-phenyl), 58.8 (s, O–*C*H$_2$–CH$_3$), 43.0 (s, NH–*C*H$_2$–CH$_2$), 24.1 (CH$_2$–*C*H$_2$–CH$_2$), 18.6 (s, O–CH$_2$–*C*H$_3$), 8.0 (s, CH$_2$–*C*H$_2$–Si) — $^{31}$P{$^{1}$H}-NMR (CD$_2$Cl$_2$): $\delta = 29.2$ (d, $^{1}J_{RhP} = 124.7$ Hz) — IR (KBr, cm$^{-1}$): 3331 [$\nu$(NH)], 1980, 1693 [$\nu$(CO)] — MS (EI); *m*/*z*: 1214 [M$^{+}$], 1186 [M$^{+}$ − CO] — Anal. Found: C, 55.79; H, 5.96; N, 4.28. Calc. for $C_{57}H_{74}ClN_4O_9P_2RhSi_2$: C, 56.31; H, 6.14; N, 4.61%.

### 4.5. General procedure for the sol–gel processing

To a solution of **2(T$^0$)**, **3(T$^0$)** in 6 ml of THF the corresponding amount of the co-condensation agent **4(D$^0$)**, **4(T$^0$)**, **5(D$^0$)**, and **5(T$^0$)**, 1.0 g (56 mmol) of H$_2$O and the catalyst tetrabutylammoniumfluoride (TBAF) (0.1 ml of a 1 M solution in THF) was added. The reaction mixture was stirred at room temperature for 24 h until a gel was formed. Subsequently the solvent was removed under reduced pressure and the crude product was dried for 2 h. After washing three times with MeOH (5 ml) and *n*-hexane (5 ml) and drying in vacuum for 4 h the xerogels were obtained as yellow powders.

*Compound* ***X2a***: Initial weight of **2(T$^0$)** 101 mg (0.2 mmol) and of **4(D$^0$)** 145 mg (0.5 mmol). Yield: 153 mg — $^{31}$P CP/MAS-NMR: $\delta = -6.3$ — $^{13}$C CP/MAS-NMR: $\delta = 156.7$ (NH–CO–NH), 139.0–118.5 (br, C-phenyl), 57.8 (O–*C*H$_2$–CH$_3$), 42.3–17.8 (br, CH$_2$ of backbone and spacer), −0.3 (Si–CH$_3$) — $^{29}$Si CP/MAS-NMR: $\delta = -4.8$ (D$^0$), −14.3 (D$^1$), −22.3 (D$^2$), −58.2 (T$^2$), −67.7 (T$^3$).

*Compound* ***X2b***: Initial weight of **2(T$^0$)** 101 mg (0.2 mmol) and of **5(D$^0$)** 184 mg (0.5 mmol). Yield: 162 mg — $^{31}$P CP/MAS-NMR: $\delta = -6.7$ — $^{13}$C CP/MAS-NMR: $\delta = 156.1$ (NH–CO–NH), 133.0–119.0 (br, C-phenyl), 57.7 (O–*C*H$_2$–CH$_3$), 38.9–17.8 (br, CH$_2$ of backbone and spacer), −0.5 (Si–CH$_3$) — $^{29}$Si CP/MAS-NMR: $\delta = -4.9$ (D$^0$), −14.4 (D$^1$), −21.9 (D$^2$), −57.5 (T$^2$), −66.8 (T$^3$).

*Compound* ***X3a***: Initial weight of **3(T$^0$)** 73 mg (0.06 mmol) and of **4(D$^0$)** 353 mg (1.2 mmol). Yield: 321 mg — $^{31}$P CP/MAS-NMR: $\delta = 29.1$ — $^{13}$C CP/MAS-NMR: $\delta = 156.0$ (NH–CO–NH), 143.8–117.6 (br, C-phenyl), 55.2 (O–*C*H$_2$–CH$_3$), 33.3–17.6 (br, CH$_2$ of backbone and spacer), −0.4 (Si–CH$_3$) — $^{29}$Si CP/MAS-NMR: $\delta = -12.3$ (D$^1$), −22.0 (D$^2$), −59.2 (T$^2$), −68.6 (T$^3$) — IR (KBr, cm$^{-1}$): 1982 [$\nu$(CO)].

*Compound* ***X3b***: Initial weight of **3(T$^0$)** 75 mg (0.06 mmol) and of **5(D$^0$)** 457 mg (1.2 mmol). Yield: 355 mg — $^{31}$P CP/MAS-NMR: $\delta = 28.9$ — $^{13}$C CP/MAS-NMR: $\delta = 156.6$ (NH–CO–NH), 139.5–118.2 (br, C-phenyl), 38.8–17.1 (br, CH$_2$ of backbone and spacer), −0.5 (Si–CH$_3$) — $^{29}$Si CP/MAS NMR: $\delta = -4.9$ (D$^0$), −14.4 (D$^1$), −21.9 (D$^2$), −57.5 (T$^2$), −66.8 (T$^3$) — IR (KBr, cm$^{-1}$): 1982 [$\nu$(CO)].

*Compound* ***X3c***: Initial weight of **3(T$^0$)** 50 mg (0.04 mmol) and of **4(T$^0$)** 269 mg (0.8 mmol). Yield: 237 mg — $^{31}$P CP/MAS-NMR: $\delta = 29.6$ — $^{13}$C CP/MAS-NMR: $\delta = 155.1$ (NH–CO–NH), 135.8–118.3 (br, C-phenyl), 31.5–12.7 (br, CH$_2$ of backbone and spacer) — $^{29}$Si CP/MAS-NMR: $\delta = -56.6$ (T$^2$), −65.6 (T$^3$) — IR (KBr, cm$^{-1}$): 1980 [$\nu$(CO)].

*Compound* ***X3d***: Initial weight of **3(T$^0$)** 75 mg (0.06 mmol) and of **5(T$^0$)** 497 mg (1.2 mmol). Yield: 385 mg — $^{31}$P CP/MAS-NMR: $\delta = 29.0$ — $^{13}$C CP/MAS-NMR: $\delta = 156.1$ (NH–CO–NH), 139.5–118.0 (br, C-phenyl), 37.4–12.8 (br, CH$_2$ of backbone and spacer) — $^{29}$Si CP/MAS-NMR: $\delta = -56.8$ (T$^2$), −65.6 (T$^3$) — IR (KBr, cm$^{-1}$): 1981 [$\nu$(CO)].

## Acknowledgements

The support of this research by the Deutsche Forschungsgemeinschaft (Graduiertenkolleg “Chemie in Interphasen” Grant No. 441/2, Bonn-Bad Godesberg) and by the Fonds der Chemischen Industrie, Frankfurt/Main is gratefully acknowledged. We thank M. Henes, Institut für Anorganische Chemie II, University of Tübingen, for IR measurements. Finally we thank Degussa AG, Germany, for a generous gift of RhCl$_3$.

## References

[1] C. Nachtigal, S. Al-Gharabli, K. Eichele, E. Lindner, H.A. Mayer, Organometallics, in press.

[2] F.R. Hartley, P.N. Vezey, Adv. Organomet. Chem. 15 (1977) 189.

[3] F.R. Hartley, Supported Metal Complexes, D. Reidel, Dordrecht, 1985.

[4] D.W. Sindorf, G.E. Maciel, J. Am. Chem. Soc. 105 (1983) 3767.

[5] S.C. Bourque, H. Alper, L.E. Manzer, P. Arya, J. Am. Chem. Soc. 122 (2000) 956.

[6] J.L.G. Fierro, M.D. Merchan, S. Rojas, P. Terreros, J. Mol. Catal. A 166 (2001) 255.

[7] P.M. Price, J.H. Clark, D.J. Macquarrie, J. Chem. Soc. Dalton Trans. (2000) 101.

[8] C. Merckle, S. Haubrich, J. Blümel, J. Organomet. Chem. 627 (2001) 44.

[9] U. Schubert, New J. Chem. 18 (1994) 1049.

[10] J. Schwarz, V.P.W. Böhm, M.G. Gardiner, M. Grosche, W.A. Herrmann, W. Hieringer, G. Raudaschl-Sieber, Chem. Eur. J. 6 (2000) 1773.

[11] I.S. Khatib, R.V. Parish, J. Organomet. Chem. 369 (1989) 9.

[12] E. Lindner, F. Auer, T. Schneller, H.A. Mayer, Angew. Chem. Int. Ed. Engl. 38 (1999) 2154.

[13] E. Lindner, A. Jäger, T. Schneller, H.A. Mayer, Chem. Mater. 9 (1997) 81.

[14] C.J. Brinker, G.W. Scherer, Sol Gel Science, Academic Press, London, 1990.

[15] B. Breitscheidel, J. Zieder, U. Schubert, Chem. Mater. 3 (1991) 559.

[16] R.J.P. Corriu, C. Hoarau, A. Mehdi, C. Reye, J. Chem. Soc. Chem. Commun. (2000) 71.

[17] E. Lindner, M. Kemmler, H.A. Mayer, P. Wegner, J. Am. Chem. Soc. 116 (1994) 348.

[18] J. Büchele, H.A. Mayer, J. Chem. Soc. Chem. Commun. (1999) 2165.

[19] E. Lindner, R. Schreiber, M. Kemmler, T. Schneller, H.A. Mayer, Chem. Mater. 7 (1995) 951.

[20] E. Lindner, T. Schneller, H.A. Mayer, H. Bertagnolli, T.S. Ertel, W. Hörner, Chem. Mater. 9 (1997) 1524.

[21] E. Lindner, A. Baumann, P. Wegner, H.A. Mayer, U. Reinöhl, A. Weber, T.S. Ertel, H. Bertagnolli, J. Mater. Chem. 10 (2000) 1655.

[22] E. Lindner, T. Schneller, F. Auer, P. Wegner, H.A. Mayer, Chem. Eur. J. 3 (1997) 1833.

[23] E. Lindner, A. Jäger, F. Auer, P. Wegner, H.A. Mayer, A. Benez, D. Adam, E. Plies, Chem. Mater. 10 (1998) 217.

[24] E. Lindner, F. Auer, A. Baumann, P. Wegner, H.A. Mayer, H. Bertagnolli, U. Reinöhl, T.S. Ertel, A. Weber, J. Mol. Catal. A 157 (2000) 97.

[25] E. Lindner, S. Brugger, S. Steinbrecher, E. Plies, M. Seiler, H. Bertagnolli, P. Wegner, H.A. Mayer, Inorg. Chim. Acta, in press.

[26] E. Lindner, T. Salesch, F. Hoehn, H.A. Mayer, Z. Anorg. Allg. Chem. 625 (1999) 2133.

[27] E. Lindner, T. Salesch, J. Organomet. Chem. 628 (2001) 151.

[28] C.A. Fyfe, Solid State NMR for Chemists, CRC Press, Gulph, ON, 1984.

[29] G. Engelhardt, D. Michel, High-Resolution NMR of Silicates and Zeolithes, Wiley, Chichester, 1987.

[30] K. Schmidt-Rohr, H.W. Spiess, Multidimensional Solid State NMR and Polymers, Academic Press, London, 1994.

[31] D.W. Sindorf, G.E. Maciel, J. Am. Chem. Soc. 105 (1983) 3767.

[32] E. Bayer, K. Albert, J. Reiners, M. Nieder, D. Müller, J. Chromatogr. 33 (1983) 197.

[33] R.K. Harris, Analyst 110 (1985) 649.

[34] E. Lindner, S. Brugger, S. Steinbrecher, E. Plies, H.A. Mayer, Z. Anorg. Allg. Chem. 627 (2001) 1731.

[35] E. Lindner, W. Wielandt, A. Baumann, H.A. Mayer, U. Reinöhl, A. Weber, T.S. Ertel, H. Bertagnolli, Chem. Mater. 11 (1999) 1833.

[36] D. Evans, J.A. Osborn, G. Wilkinson, J. Chem. Soc. A (1968) 3133.

[37] M. Beller, B. Cornils, C.D. Frohning, C.W. Kohlpaintner, J. Mol. Catal. A 104 (1995) 17.

[38] L.A. van der Veen, P.C.J. Kamer, P.W.N.M. van Leeuwen, Organometallics 18 (1999) 4765.

[39] H.-J. Egelhaaf, E. Holder, P. Herman, H.A. Mayer, D. Oelkrug, E. Lindner, J. Mater. Chem. 11 (2001) 2445.

[40] R.S. Aujla, R.K. Harris, K.J. Packer, M. Parameswaran, B.J. Say, A. Bunn, M.E.A. Cudby, Polym. Bull. 8 (1982) 253.

[41] G. Giordano, R.H. Crabtree, Inorg. Synth. 28 (1990) 88.

[42] O. Herd, A. Heßler, M. Hingst, M. Trapper, O. Stelzer, J. Organomet. Chem. 522 (1996) 69.